

# Computational Modeling of Translucent Concrete Panels

Aashish Ahuja<sup>1</sup>; Khalid M. Mosalam, M.ASCE<sup>2</sup>; and Tarek I. Zohdi<sup>3</sup>

**Abstract:** The last decade has witnessed a heightened interest in making buildings more sustainable, which has been fueled largely by the increase in energy costs and advancements in manufacturing technology. Lighting consumes a substantial amount of this energy, making it necessary to look for alternative technology that depends more on natural lighting. This study investigated a novel building envelope material that consists of optical fibers embedded in concrete. The fibers are used to channel solar radiation into the building to reduce the dependence on artificial lighting especially during peak time. This paper presents a geometrical ray-tracing algorithm to simulate light transmission properties of the proposed translucent concrete panel. It was concluded that a tilt angle of 30° for the panel transmits the maximum amount of light among all the tilt angles considered. Using this tilt angle, the rate at which sunlight radiation is absorbed by the panel was calculated, and a preliminary study was conducted to estimate the solar heat gain coefficient of the panel for possible use in place of a glazing material by the construction industry. DOI: 10.1061/(ASCE)AE.1943-5568.0000167. © 2014 American Society of Civil Engineers.

**Author keywords:** Concrete panel; Daylight capture; Energy efficiency; Ray tracing; Simulations; Solar heat gain; Structural wall; Translucent concrete.

## Introduction

Buildings (commercial and residential) consume almost 41% of the total energy that is available for use in the United States. A large part of this energy, in the form of electricity, is used solely in artificially lighting the indoors of buildings (DOE 2011). The electric energy is derived primarily from thermal power plants that are not clean sources and contribute to greenhouse gas emissions. An innovation like translucent concrete (TC) captures and delivers daylight into buildings, which could reduce our dependence on indoor lighting and save electricity. Such technology can be constructed as a part of a building envelope (i.e., wall and roof), because it satisfies requirements that are usually set apart (Mosalam et al. 2013): (1) envelope behaving as a structural subsystem, (2) construction procedure is simple and scalable, and (3) movable and mechanized parts are avoided. Compared with a traditional electric lighting system, illuminating the indoors with daylight also creates a more appealing and healthy environment for building occupants (Edwards and Torcellini 2002).

In this paper, the authors used available sunlight data in estimating the light-transmitting capabilities of TC. The computational model of a TC panel consists of a grid of plastic optical fibers (OFs) embedded in concrete, allowing light to be transmitted through the otherwise opaque panel. Daily simulations were carried out at intervals of 30 min between 8 a.m. and 5 p.m. The results for the whole year were collected to infer the panel's transmissibility of direct and diffused sunlight. Based on the simulation results, the heating rate of the panel was estimated for different times of the year.

<sup>1</sup>Ph.D. Candidate, Dept. of Mechanical Engineering, Univ. of California, Berkeley, CA 94720-1740. E-mail: aashishahuja@berkeley.edu

<sup>2</sup>Professor, Dept. of Civil and Environmental Engineering, Univ. of California, Berkeley, CA 94720-1710 (corresponding author). E-mail: mosalam@berkeley.edu

<sup>3</sup>Professor, Dept. of Mechanical Engineering, Univ. of California, Berkeley, CA 94720-1740. E-mail: zohdi@me.berkeley.edu

Note. This manuscript was submitted on March 18, 2014; approved on October 20, 2014; published online on November 11, 2014. Discussion period open until April 11, 2015; separate discussions must be submitted for individual papers. This paper is part of the *Journal of Architectural Engineering*, © ASCE, ISSN 1076-0431/B4014008(8)/\$25.00.

## Previous Work on TC

In 2001, Hungarian architect Aron Losonzi invented LiTraCon, the first commercially available form of TC. It was a combination of optical fibers and fine concrete, combined in such a way that the material was both internally and externally homogeneous. It was manufactured in blocks and used primarily for decoration. The current price of a LiTraCon block (100 mm thick) is approximately 2,140 Euro/m<sup>2</sup> (Ex Works), which makes it prohibitively expensive and difficult to commercialize. During the World Expo 2010 Shanghai China, Italy modeled its pavilion out of TC using approximately 4,000 blocks. The blocks were rather heavy to be used as a facade subsystem in buildings. Another product featured plastic fibers arranged in a grid, namely Pixel Panels, developed by Bill Price of the University of Houston. These panels transmitted light in a pattern resembling thousands of tiny stars in the night sky. University of Detroit Mercy also developed a process to produce translucent panels made of portland cement and sand and reinforced it with a small amount of chopped fiberglass. These panels, which were only 2.5 mm thick at their centers, were thin enough to be translucent under direct light.

The primary focus of the TC technology previously has been on its aesthetic appeal and its application in artistic design. Recently, He et al. (2011) published a study on smart TC, which experimentally explored the light emission properties of TC in the laboratory. Building on his research, this study took a step further by modeling light transmission and studying heating rate of the TC panel when exposed to sunlight throughout the year. Interestingly, development of light-transmitting facades is gaining more interest. Recently, a study on a novel translucent facade made from organic materials like sucrose was published (Gutierrez and Zohdi 2014).

## Theory and Modeling

### *Illumination and Irradiation Calculations for the TC Panel*

The sky is described as a Perez model (Perez et al. 1987) that estimates the global irradiance (or illuminance) on a tilted surface. Global irradiance ( $G$ ) is the sum of direct horizontal ( $G_b$ ) and diffuse ( $G_d$ ) components of the sunlight irradiance, given as

$$G = G_b \frac{\cos \theta}{\cos \theta_z} + G_d \quad (1)$$

where  $\theta$  = angle between the sun direction and normal to the panel surface; and  $\theta_z$  = solar zenith angle.

One can calculate  $\theta$  (Fig. 1) for a south-facing panel with a solar azimuth angle,  $a_z$ , and tilt angle,  $\beta$ , as

$$\theta = \cos^{-1}(\cos \theta_z \cos \beta - \sin \theta_z \sin \beta \cos a_z) \quad (2)$$

Weather stations in the United States record the direct beam ( $G_n = G_b/\cos \theta_z$ ) irradiance component of sunlight, which is the direct horizontal flux of the sun at zenith. Accordingly, Eq. (1) is modified to yield

$$G = G_n \cos \theta + G_d \quad (3)$$

The total irradiance ( $G$ ) on a tilted surface also includes an additional component owing to radiation reflected from the ground ( $G_r$ ). This reflected radiation rarely accounts for a significant part of the sunlight striking a surface and, hence, is ignored in Eq. (3). Under the Perez sky model assumption, the diffuse solar radiation ( $G_d$ ) on a tilted surface is calculated as the sum of the following components (Fig. 2):

1. Isotropic radiation ( $I_{\text{dome}}$ ), which is uniformly distributed over the sky vault.
2. Radiations from circumsolar disk ( $I_{\text{circum}}$ ) and sky horizon ( $I_{\text{hor}}$ ), which cause anisotropic distribution of diffused light.

The circumsolar disk subtends a half-angle of  $25^\circ$  around the sun produced from forward scattering by aerosols and multiple Rayleigh scattering. A bright band of  $6.5^\circ$  elevation develops near the horizon because of sunlight retroscattering. The contribution of each component (isotropic, circumsolar, or sky horizon) in the final equation for diffused light depends on the sky brightness factor,  $\Delta$ , atmospheric clearness,  $\epsilon$ , and zenith angle,  $\theta_z$ . Hence,  $G_d$  for a tilted surface can be expressed as

$$G_d = G_d(0) \left[ (1 - F_1) \frac{1 + \cos \beta}{2} + F_1 \frac{\cos \theta}{\cos \theta_z} + F_2 \sin \beta \right] \quad (4)$$

where

$$F_1(\epsilon) = f_{11} + f_{12}\Delta + f_{13}\theta_z, \quad F_2(\epsilon) = f_{21} + f_{22}\Delta + f_{23}\theta_z \quad (5)$$

and

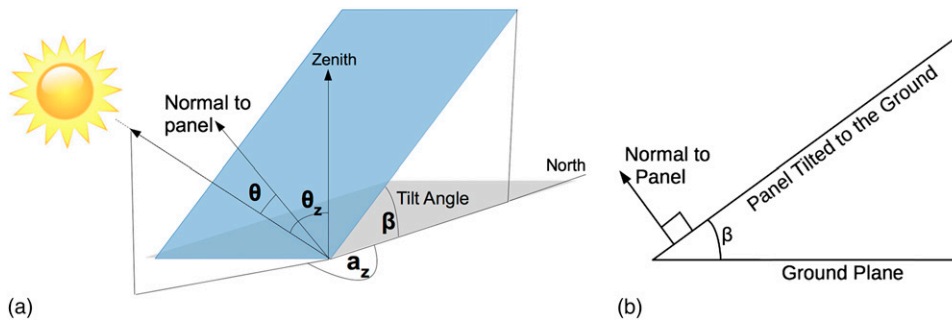


**Fig. 1.** Setup for a tilted TC panel simulation: (a) definition of geometric parameters; (b) side view of the panel

$$\Delta = \frac{mG_d(0)}{G_{\text{etr}}}, \quad \epsilon = \frac{G_d(0) + G_n(0)}{G_d(0)} \quad (6)$$

where  $G_d(0)$  and  $G_n(0)$  = diffused and direct beam irradiances, respectively, on a horizontal plane;  $m$  = atmospheric air mass; and  $G_{\text{etr}}$  = extraterrestrial radiation. The weather file (Crawley et al. 1999) only reports the measured value for extraterrestrial solar irradiation (watts per square meter) but does not contain the corresponding illuminance (lx) value. Extraterrestrial solar illuminance (lx) is estimated analytically by considering the elliptical orbit of the earth around the sun

$$G_{\text{etr}} = 133,100 \left[ 1 + 0.034 \cos \frac{2\pi(N-2)}{365} \right] \quad (7)$$

where  $N$  = Julian date.

The coefficients  $f_{ij}$  are dependent on  $\epsilon$  and are given elsewhere (Perez et al. 1987, Table 1). The atmospheric air mass is a measure of the path length of solar radiation through the atmosphere. The equation of  $m$  in Kasten and Young (1989) is used widely by engineers and was adopted in this study

$$m = \frac{1}{\cos(\theta_z) + 0.50572 \left( 96.07995 - \theta_z \frac{180}{\pi} \right)^{-1.6364}} \quad (8)$$

## Modeling

For simulation purposes, a TC panel was modeled as a cuboid with dimensions  $0.3 \times 0.3 \times 0.1$  m (Fig. 3). The transparency of the TC panel was varied by changing the volumetric ratio of optical fibers embedded in the concrete. The light travels in the core of the optical fibers, which is made up of polymethyl methacrylate (PMMA). The core is surrounded by a thin layer of perfluorinated (PF) polymer known as the cladding. The cladding protects the core and allows light to propagate by total internal reflection at the core-cladding interface.

## Light Transmission through the Optical Fibers

A ray of light incident on an optical fiber in the TC panel undergoes three noticeable light phenomena: reflection and refraction on its top surface and total internal reflection (TIR) along the inside walls of the fiber. The amount of light reflected after striking the top of optical fibers is given as [for derivation, see Zohdi (2012) and Gross (2005)]

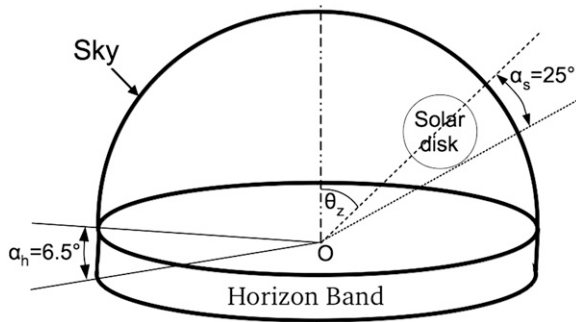


**Fig. 2.** Description of Perez circumsolar radiation and horizon radiation band

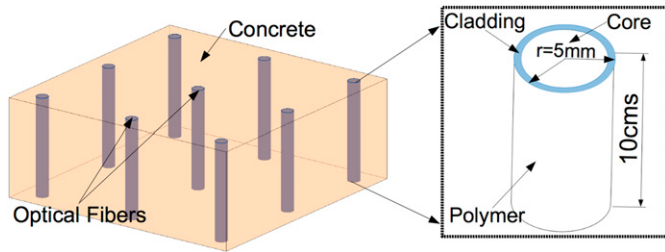


**Fig. 3.** A computational model of TC panel with embedded optical fibers

$$R = \frac{1}{2} \left[ \left( \frac{\hat{n}^2 \cos \theta_i - \sqrt{\hat{n}^2 - \sin^2 \theta_i}}{\hat{\mu}} \right)^2 + \left( \frac{\cos \theta_i - \frac{1}{\hat{\mu}} \sqrt{\hat{n}^2 - \sin^2 \theta_i}}{\cos \theta_i + \frac{1}{\hat{\mu}} \sqrt{\hat{n}^2 - \sin^2 \theta_i}} \right)^2 \right] \quad (9)$$

where  $0 \leq R \leq 1$  for an angle of incidence  $\theta_i$ ;  $\hat{\mu} = \mu_t / \mu_i = 1$  [ $\hat{\mu}$  is the ratio of magnetic permeabilities for transmission and incident media; whereas most polymers or ceramics are nonmagnetic and have  $\hat{\mu} \approx 1$ , materials like  $\gamma\text{-Fe}_2\text{O}_3$  (Dagani 1992) are magnetic and optically transmitting but only exist at the nanometer scale]; and  $\hat{n} = n_t / n_i$  ( $\hat{n}$  is the ratio of refractive indexes for transmission and incident media). The light that is refracted into the optical fibers may or may not undergo TIR. For the TIR to occur within an optical fiber

$$n_{\text{core}} \sin \theta_i > n_{\text{cladding}} \quad (10)$$

where  $n_{\text{core}}$  and  $n_{\text{cladding}}$  = refractive indexes for the core and cladding materials of the optical fiber, respectively. Light rays that do not obey this condition [Eq. (10)] are dissipated as heat within the fiber.

### Intrinsic Losses in Optical Fibers

An optical fiber comprises a PMMA core protected by a cladding of small thickness. The refractive index of the cladding is less than that of the core, a requirement necessary to initiate TIR. Also, in the case of plastic optical fibers, refractive indexes vary slightly over a range of wavelengths (Ishigure et al. 1996). This study used a refractive index of 1.49 for the core and 1.40 for the cladding, which were provided by the manufacturer of the considered type of fiber with a numerical aperture (N.A.) ( $= \sqrt{n_{\text{core}}^2 - n_{\text{cladding}}^2}$ ), of 0.51. As light travels through the core, it suffers two types of intrinsic losses (Zubia and Arrue 2001) as follows:

1. Light scattering due to fluctuation in density and composition of material. For PMMA, the loss factor is  $\alpha_R = 13 \times (633/\lambda)^4$  dB/km (Kaino 1997).
2. Light absorption from electronic transitions between the excited and the ground states (Urbach's rule). Loss factor,  $\alpha_e = 1.58 \times 10^{-12} \exp(1.15 \times 10^4/\lambda)$  dB/km (Kaino 1985).

Light absorption leads to heating up of the optical fiber, whereas the radiation dissipated via the scattering process is rejected by the optical fiber. The significant terrestrial radiation (280–4,000 nm) is broken into three spectra: (1) ultraviolet (UV) range (280–380 nm), (2) visible light (380–780 nm), and (3) infrared (IR) range (780–4,000 nm) of solar radiation. To calculate the intrinsic transmittance of a PMMA optical fiber with rays having an average optical path length of  $L$  (in kilometers), one applies Eq. (11) (Kato and Nakamura 1976) to each spectrum

$$T(L) = \frac{\int_{\lambda_1}^{\lambda_2} E_o(\lambda) \exp[-(\alpha_R + \alpha_e)L] d\lambda}{\int_{\lambda_1}^{\lambda_2} E_o(\lambda) d\lambda} \quad (11)$$

where the solar spectral distribution as a function of the wavelength ( $\lambda$ ) is defined as  $E_o(\lambda) = C_1 / \{\lambda^5 [\exp(C_2/\lambda) - 1]\}$  with  $C_1 = 8.097 \times 10^{-21} \text{ Wm}^2$  and  $C_2 = 2.497 \times 10^{-6} \text{ m}$ . In the current model, the intrinsic transmittances for a 10-cm-long fiber (Fig. 3) with a path length of  $1.25 \times 10^{-4} \text{ km}$  was computed using Gaussian quadrature

$$T_{\text{UV}} = 0.78; \quad T_{\text{Visible}} = 0.99; \quad T_{\text{IR}} = 0.99 \quad (12)$$

Because the length of the selected optical fiber was small, the reduction in transmittance ratios [Eq. (12)] across different spectra primarily was due to absorption. Attenuation due to scattering of light is negligible in this case, but increases exponentially for a longer fiber.

### Modified Perez Model for the TC Panel

The TC panel contains cylindrical optical fibers that exhibit a limited acceptance cone for light transmission (Fig. 4). This loss of light is in addition to the light reflection at the top and bottom surfaces and losses due to intrinsic effects of fiber. Thus, all components of incident global irradiation ( $G$ ) would not be transmitted through the fiber equally. The ratio of each component (direct, isotropic, etc.) that is transmitted through a tilted TC panel is calculated using geometrical ray tracing, which is explained subsequently. These ratios are inculcated in the modified form of Eqs. (3) and (4) to give

$$G' = D_n G_n \cos \theta + G'_d$$

$$G'_d = G_d(0) \left[ D_i(1 - F_1) \frac{1 + \cos \beta}{2} + D_c F_1 \frac{\cos \theta}{\cos \theta_z} + D_h F_2 \sin \beta \right] \quad (13)$$

where  $G'$  and  $G'_d$  = global and diffused irradiance (or illuminance), respectively, collected on a surface adjoining and parallel to the TC panel; and  $D_n, D_i, D_c,$  and  $D_h$  = averaged panel transmittance ratios for their respective global irradiation components. Finally,  $G'$  and  $G'_d$  are multiplied by the area of the TC panel ( $0.09 \text{ m}^2$  in this case) to give the total luminous flux (in lumens) value.

### Geometrical Ray Tracing

Ray-tracing methods begin by representing wavefronts as an array of discrete rays. Geometrically, one proceeds by tracking each ray as it changes trajectories. On encountering a surface, the intersection

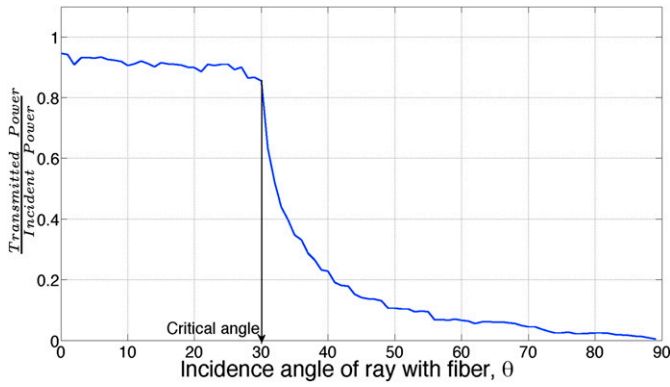


**Fig. 4.** Performance of optical fiber deteriorates as light rays subtend larger angles with fiber

point is either determined analytically (in case the surface geometry is simple, such as a sphere or polygon) or using some numerical method, like Newton's method. Next, Fresnel's laws are applied at the intersection point and the outgoing ray (reflected or refracted) is calculated. Ray-tracing methods, in general, are well suited for the computation of scattering in complex systems that are difficult to mesh/discretize. It is assumed that the length scale of the surface features are large enough relative to the optical wavelength of sunlight ( $280 \text{ nm} \leq \lambda \leq 4,000 \text{ nm}$ ) and the reflections at the surface are specular, allowing use of the ray-tracing theory (Zohdi 2012). A detailed algorithm for ray tracing using the modified Perez sky model is given in Fig. 5.

## Rate of Heat Absorption for the TC Panel

### Terrestrial Radiation

Outside the Earth's atmosphere, the distribution of solar flux with respect to the wavelength is referred to as AM0 meaning zero atmospheres. The authors use AM1.5 for calculating the spectrum for terrestrial global irradiation. AM1.5 is also the standard for testing photovoltaic (PV) panels designed for terrestrial use. As mentioned previously, the band of significant terrestrial radiation (280–4,000 nm) is divided into three ranges (UV, visible light, and IR). The entire solar spectrum for terrestrial irradiation is compiled in ASTM G173-03(2012) (ASTM 2012). The contribution of each component is calculated using Simpson's method by integrating over discrete flux values for all wavelengths. It is determined that AM1.5 global irradiation mainly consists of visible light (53.49%), followed by IR (43.23%), and UV radiation (3.28%).

### Heat Absorption and Reflectivity of the TC Panel

The fraction of sunlight (diffuse and direct irradiation) that is absorbed by concrete and optical fibers contributes to the net heating of the TC panel. The energy balance equation is applied to calculate the amount of heat absorbed by the panel, assuming that all the incident radiation is stored in the panel, while ignoring conduction and convection. Thus

$$m_{TC} C_{TC} \frac{dT}{dt} = E^{ab} A \quad (14)$$

where  $m_{TC}$  = mass of the TC panel;  $C_{TC}$  = heat capacity of the TC panel;  $dT/dt$  = heating rate ( $^{\circ}\text{C/s}$ );  $A$  = total TC panel area; and  $E^{ab}$  = fraction of the global irradiation ( $G$ ) that is absorbed by the panel

( $\text{W/m}^2$ ). The concrete part of the TC panel considered in this paper was assumed to be Leadership in Energy and Environmental Design (LEED) certified, which sets its surface absorptivity value to  $\chi_c = 0.36$  throughout the solar spectrum. Light rays that do not follow the condition for the TIR [Eq. (10)] dissipate as heat inside the optical fibers; moreover, fibers are heated up owing to Urbach's rule [Eq. (12)]. The combined heating of concrete and optical fibers gives the final value of  $E^{ab}$ .

The calculations for heat absorption by the TC panel can be summed up by the following equations:

$$E^{ab} = A_c \chi_c G + A_f E_{\text{direct}} + A_f E_{\text{diffused}} \quad (15)$$

where

$$E_{\text{direct}} = \chi_1 G_n \cos \theta$$

$$E_{\text{diffused}} = G_d(0) \left[ \chi_2 (1 - F_1) \frac{1 + \cos \beta}{2} + \chi_3 F_1 \frac{\cos \theta}{\cos \theta_z} + \chi_4 F_2 \sin \beta \right] \quad (16)$$

where  $A_c$  and  $A_f$  = surface areas of concrete and fibers, respectively. The coefficients  $\chi_i$  ( $i = 1, 2, 3, 4$ ) in the heat absorption [Eq. (16)] are obtained slightly differently from the corresponding  $D$  coefficients used in the illuminance [Eq. (13)]. Illuminance only pertains to the visible region of light spectrum, whereas in heat calculations, one has to consider absorption of light rays for each spectrum. The flowchart (Fig. 6) gives the procedure to obtain the  $\chi_i$  ( $i = 1, 2, 3, 4$ ) coefficients to apply Eq. (16).

Expanding the coefficient of the derivative in the left-hand side of Eq. (14) yields

$$m_{TC} C_{TC} \approx [(\rho C)_c A_c + (\rho C)_f A_f] d \quad (17)$$

where  $d$  = thickness of the TC panel; and  $\rho$  = material density. Solving for  $dT/dt$

$$\frac{dT}{dt} = \frac{E^{ab} A}{[(\rho C)_c A_c + (\rho C)_f A_f] d} \quad (18)$$

Normalized effective heating rate,  $H^*$ , is calculated to compare the thermal mass property of the TC panel with that of a pure concrete panel with similar dimensions

$$H^* = \frac{(dT/dt)|_{v_2}}{(dT/dt)|_{v_2=0}} \quad (19)$$

where  $v_2$  = volumetric ratio defined as  $A_f/A$ . Further, the authors estimated the interior solar heat gain due to an optical fiber, which is based on the approach defined in Li and Lam (2000). It is calculated as  $\dot{q}$  (in watts per square meter)

$$\dot{q} = [1 - \tau_1 + (N_i - 1)\chi_1] G_n \cos \theta$$

$$+ G_d(0) \left\{ [1 - \tau_2 + (N_i - 1)\chi_2] (1 - F_1) \frac{1 + \cos \beta}{2} + [1 - \tau_3 + (N_i - 1)\chi_3] F_1 \frac{\cos \theta}{\cos \theta_z} + [1 - \tau_4 + (N_i - 1)\chi_4] F_2 \sin \beta \right\} \quad (20)$$

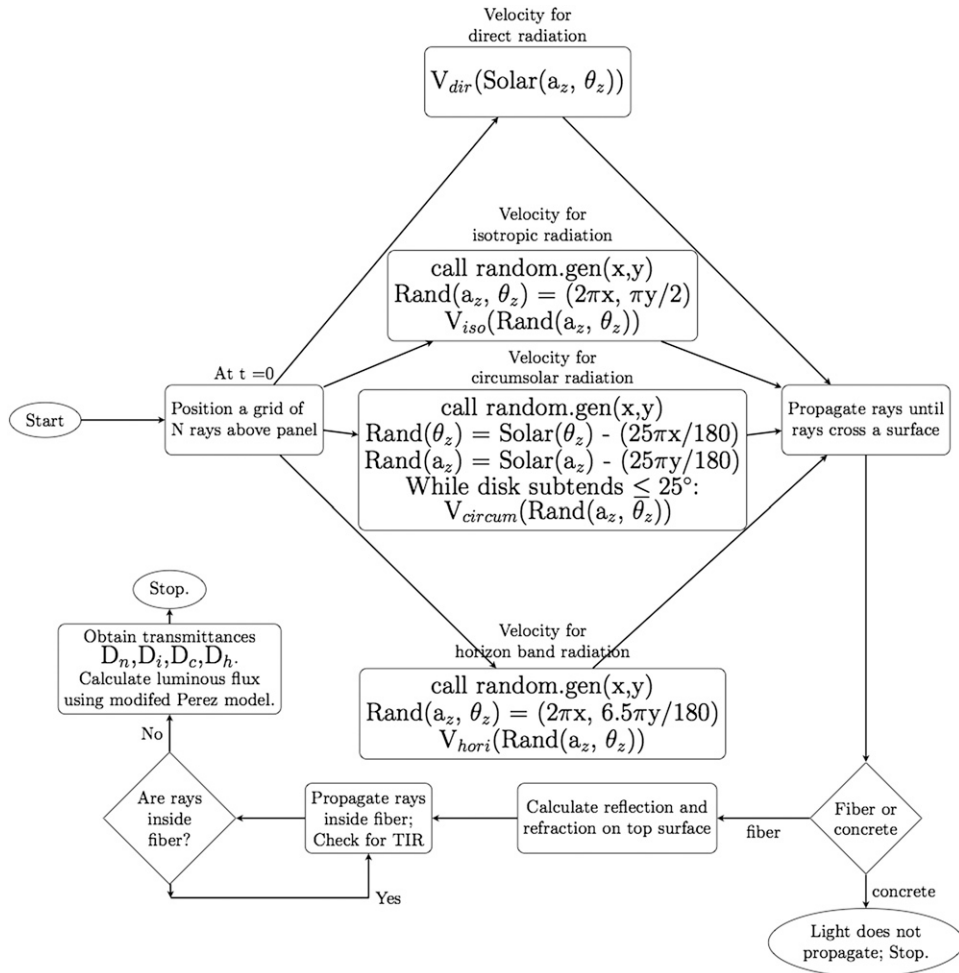


**Fig. 5.** Algorithm to calculate the total luminous flux emitted by a TC panel

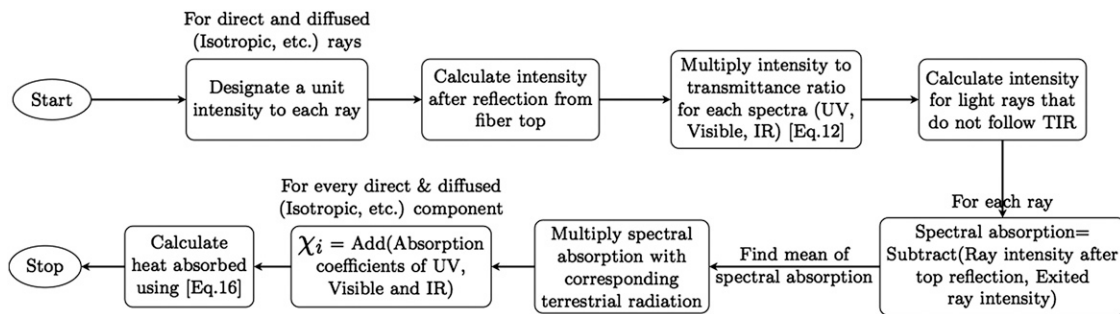


**Fig. 6.** Algorithm to calculate the heat absorption by the TC panel

where  $\tau_i$  ( $i = 1, 2, 3, 4$ ) = averaged percentage of light reflected from the top of fibers;  $N_i$  = inward flowing fraction of the absorbed radiation; and  $\chi_i$  ( $i = 1, 2, 3, 4$ ) = coefficients defined previously. The inward flowing fraction of solar radiation is expressed as

$$N_i = h_i / (h_i + h_o) \quad (21)$$

where  $h_i$  and  $h_o$  = heat transfer coefficients on the exposed interior and exterior surfaces of the facade, respectively. A value of  $h_i = 8.29 \text{ W}/(\text{m}^2 \cdot \text{K})$  is recommended for building design by the American Society of Heating, Refrigerating and Air-Conditioning

Engineers (ASHRAE). To estimate the outdoor convective coefficient,  $h_o$ , the authors referred to the average monthly wind speeds,  $V_r$  (meters per second), listed in the typical meteorological year (TMY) weather file. The expression proposed in Loveday and Taki (1996) calculates  $h_o$  from surface wind speed,  $V_s$  (meters per second), as

$$h_o = 16.21 V_s^{0.452} \quad (22)$$

where  $V_s = 0.68 V_r - 0.5$ .

Other parameter values used for calculation purposes are the following: density of fiber,  $1,170 \text{ kg}/\text{m}^3$ ; density of concrete,

2,320 kg/m<sup>3</sup>; specific heat of fiber, 1,260 J/kg · K; and specific heat of concrete, 750 J/kg · K.

## Results and Discussion

The introduction of effective daylight responsive systems can reduce the operating costs of conventional lighting systems by 31% on an annual basis (Onaygil and Güler 2003). Moreover, the proposed TC panel contains multimode optical fibers that cause dispersion of light rays (Ghatak and Thyagarajan 1998) and shield the occupants from direct glare and visual discomfort.

For this research, the authors simulated a south-facing TC panel in Berkeley, California. The weather conditions were adapted from the data available in the TMY file for Oakland, California, which is located about 30 km from the site and fairly experiences the same weather conditions as Berkeley. The TC panel with a fiber volumetric ratio of 10.56% was simulated for multiple tilt angles (0–60° in intervals of 5°) to compute an angle that, on average for the panel, would transmit maximum light for the whole year. Both Figs. 7(a and b) use different metrics to compare the effects of the tilt angles over the year. It was not possible to select the optimal tilt angle from visual inspection of the graphs. Instead the areas under the curves in Fig. 7(b) were calculated to conclude that a tilt angle,  $\beta^* = 30^\circ$ , transmits the maximum luminous flux. The luminous flux values for the entire year for this optimal tilt angle were arranged in eight bins (Fig. 8), according to the atmospheric clearness factor,  $\varepsilon$ , defined previously,

i.e.,  $\varepsilon = 1-8$ . It was observed that, for days with overcast skies, luminous flux values were low and almost independent of the solar altitude. The dependence of flux on the solar altitude became stronger as the sky became clearer and less turbid. To plot a nonlinear best-fit curve through these data points, the authors used the robust loess scheme with a spread fraction of 0.35 (Jacoby 2000). In general, Berkeley and the surrounding Bay area experience very few days of highly clear skies, which is represented in Fig. 8(h).

The optimal tilt angle was used to model several TC panels with various fiber volumetric ratios to estimate their effective heating rate,  $H^*$  (Fig. 9). In general, it was observed that increasing the volumetric ratio of fibers in the panel reduced the rate of heat buildup during the middle of the day. For the tilt angle chosen, the heat buildup was lowest during solar noon when the position of the sun in the sky was the highest. On the contrary, the value of  $H^*$  grew during morning and late afternoon hours, as the majority of the incident sunlight was absorbed in the fiber instead of being transmitted. It is likely that, during these hours, the direct radiation,  $G_n$ , falls outside the acceptance range of the optical fibers. An exception was on the morning of March 21 (between 10 a.m. and 12 p.m.) when all the plots were close to each other. This was due to cloudy conditions ( $\varepsilon$  Bin 3) that blocked direct radiation. The weather cleared up later in the day. Thus, the presence of cloud cover also influences the heat absorption by the TC panel.

It is important to optimize the ratio of fibers inside the TC panel to minimize the introduction of unwanted heat into the building, while ensuring that sufficient visible light is available for acceptable

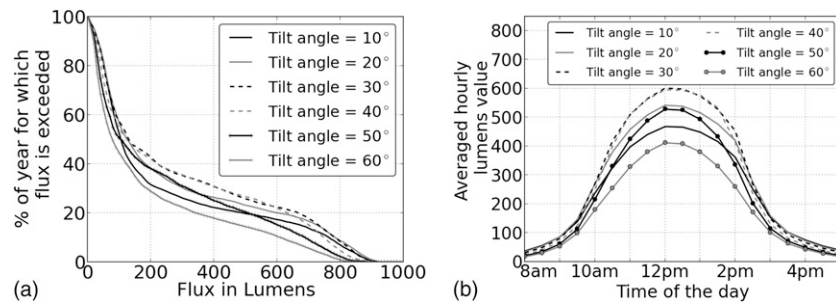


**Fig. 7.** Calculations of luminous flux for a fiber volume ratio of 10.56% based on daytime (8 a.m. to 5 p.m.): (a) luminous flux availabilities as a percentage of a non-leap year such that a flux value is exceeded; (b) average luminous flux calculated for each hour of the whole year

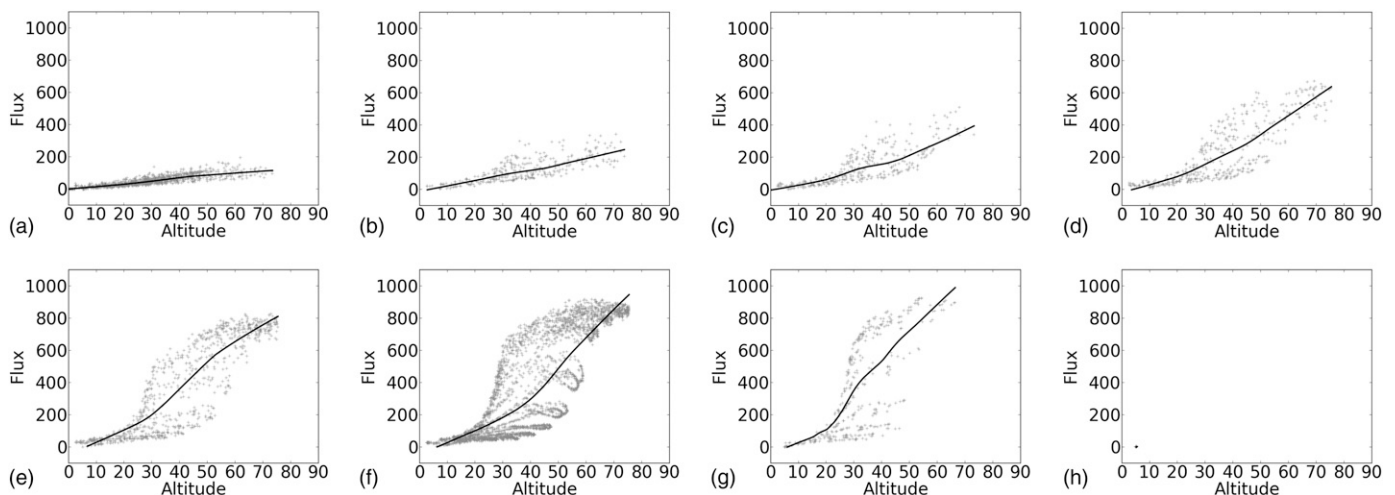


**Fig. 8.** Variation of the luminous flux with solar altitude for atmospheric clearness,  $\varepsilon$ , in (a) Bin 1; (b) Bin 2; (c) Bin 3; (d) Bin 4; (e) Bin 5; (f) Bin 6; (g) Bin 7; (h) Bin 8

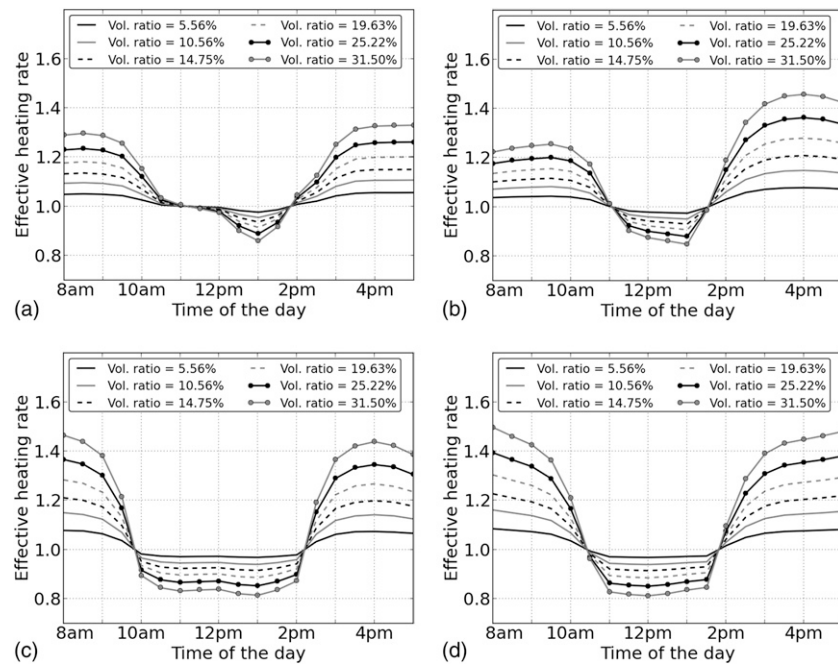


**Fig. 9.** Effective heating rate,  $H^*$ , for equinoxes and solstices: (a)  $H^*$  for March 21; (b)  $H^*$  for June 21; (c)  $H^*$  for September 21; (d)  $H^*$  for December 21

human comfort and productivity. Fig. 10 compares the solar heat gain in watts per square meter due to only optical fibers in a TC panel to a LEED-certified window for Berkeley (fenestration ratings for south/central regions apply) having a solar heat gain coefficient (SHGC) of 0.4 (Kruger and Seville 2013). As observed in Fig. 10, a TC panel admits more heat than a high-performance window during the year, which is helpful in reducing heating loads during winters, but potentially increases the cooling load for the air conditioning unit of the building during summer months. As a future extension of the study, the authors are planning to apply reflective coatings on the top of optical fibers to reflect away heat (primarily infrared) to reduce the solar heat gain in the building.

## Conclusions and Limitations of the Study

The TC panels have the distinct property of daylight transmission, which makes them useful for energy-efficient building envelopes. The use of these panels in a building can be considered as a forward step in saving energy and earning LEED credits, which presently require daylighting for at least 75% of the occupied spaces (Kubba 2010). Moreover, careful use of daylighting can contribute to occupant well-being and productivity. This paper presents a method to calculate the amount of sun radiation that enters the interior of a building by exploring the light transmission properties of the TC panel. This will help in quickly analyzing the performance of a panel in different locations, and, based on the results, the designer can make rational decisions regarding the volumetric ratio/size of fibers and the orientation of the panel during the construction phase. Additionally, one could include the value of solar heat gain, which affects the design of the HVAC system and the thermal comfort of building occupants.

This study only focused on simulating the light-transmitting abilities of this new structural element, namely the TC panel. The authors believe that, in its present form, such panels can be used in the wall or roof assembly of a building. However, the issues regarding fulfillment of building code requirements were not resolved but are being explored as an extension of this research. The simulation engine

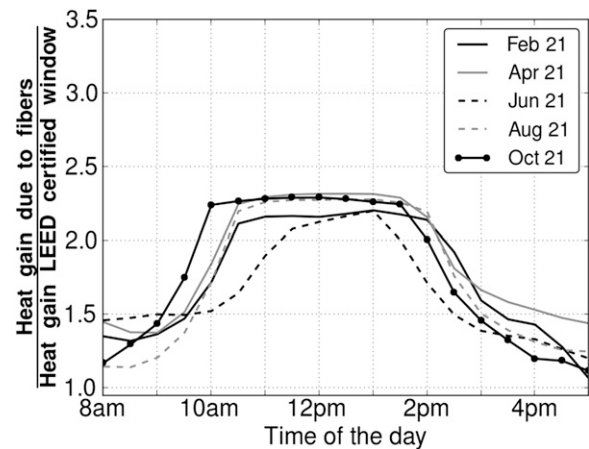


**Fig. 10.** Solar heat gain from optical fibers compared to that of a LEED-certified window

used for calculations was developed for this study and can be further expanded to interface with popular engines like *Radiance 4.2* (Ward 1994) and *EnergyPlus 8.2*. The advances in computational power have allowed one to readily parallelize ray tracing and proceed with either of the following two ways to exploit parallelism (Zohdi 2012): (1) by assigning each processor a certain number of rays and tracking their interaction with the TC panel; or (2) by dividing the whole panel into subblocks, which can represent different TC panel designs, to achieve global optimization of a large building envelope system.

## Acknowledgments

The presented research was funded by the Republic of Singapore's National Research Foundation through a grant to the Berkeley Education Alliance for Research in Singapore (BEARS) for

Singapore-Berkeley Building Efficiency and Sustainability in the Tropics (SinBerBEST) program. BEARS has been established by the University of California, Berkeley, as a center for intellectual excellence in research and education in Singapore. The authors also thank Alex Mead, Bhavesh Patel, and Zeyad Zaky for their assistance in the revision of the paper.

## References

- ASTM. (2012). "Standard tables for reference solar spectral irradiances: Direct normal and hemispherical on 37° tilted surface." *G173-03(2012)*, West Conshohocken, PA.
- Crawley, D., Hand, J., and Lawrie, L. (1999). "Improving the weather information available to simulation programs." *Proc., Building Simulation 1999*, International Building Performance Simulation Association, Ottawa.
- Dagani, R. (1992). "New material is optically transparent, magnetic at room temperature." *Chem. Eng. News*, 70(29), 20–21.
- DOE. (2011). *2010 Buildings energy data book*, Energy Efficiency & Renewable Energy, Washington, DC.
- Edwards, L., and Torcellini, P. (2002). "A literature review of the effects of natural light on building occupants." *Technical Rep. NREL/TP-550-30769*, National Renewable Energy Laboratory, Golden, CO.
- EnergyPlus 8.2* [Computer software]. Washington, DC, DOE.
- Ghatak, A., and Thyagarajan, K. (1998). *Introduction to fiber optics*, Cambridge University Press, Cambridge, U.K.
- Gross, H. (2005). "Raytracing." *Handbook of optical systems: Fundamentals of Technical Optics*, Vol. 1, Wiley-VCH, Weinheim, Germany, 173–228.
- Gutierrez, M. P., and Zohdi, T. I. (2014). "Effective reflectivity and heat generation in sucrose and PMMA mixtures." *Energy Build.*, 71(Mar), 95–103.
- He, J., Zhou, Z., Ou, J., and Huang, M. (2011). "Study on smart transparent concrete product and its performances." *Proc., 6th Int. Workshop on Advanced Smart Materials and Smart Structures Technology*, Asian-Pacific Network of Centers for Research in Smart Structure Technology (ANCRISST), Harbin Institute of Technology, Harbin, China.
- Ishigure, T., Nihei, E., and Koike, Y. (1996). "Optimum refractive-index profile of the graded-index polymer optical fiber, toward gigabit data links." *Appl. Opt.*, 35(12), 2048–2053.
- Jacoby, W. G. (2000). "Loess: A nonparametric, graphical tool for depicting relationships between variables." *Elect. Stud.*, 19(4), 577–613.
- Kaino, T. (1985). "Absorption losses of low loss plastic optical fibers." *Jpn. J. Appl. Phys.*, 24(12), 1661–1665.
- Kaino, T. (1997). "Linear optical properties of organic molecular solids." Chapter 7, *Organic molecular solids: Properties and applications*, W. Jones, ed., CRC Press, Boca Raton, FL, 201–242.
- Kasten, F., and Young, A. T. (1989). "Revised optical air mass tables and approximation formula." *Appl. Opt.*, 28(22), 4735–4738.
- Kato, D., and Nakamura, T. (1976). "Application of optical fibers to the transmission of solar radiation." *J. Appl. Phys.*, 47(10), 4528–4531.
- Kruger, A., and Seville, C. (2013). "Fenestration." *Green building: Principles and practices in residential construction*, Delmar, Cengage Learning, Clifton Park, NY.
- Kubba, S. (2010). *LEED practices, certification, and accreditation handbook*, Butterworth-Heinemann, Oxford, U.K.
- Li, D. H., and Lam, J. C. (2000). "Solar heat gain factors and the implications to building designs in subtropical regions." *Energy Build.*, 32(1), 47–55.
- Loveday, D. L., and Taki, A. H. (1996). "Convective heat transfer coefficients at a plane surface on a full-scale building facade." *Int. J. Heat Mass Transfer*, 39(8), 1729–1742.
- Mosalam, K. M., Casquero-Modrego, N., Armengou, J., Ahuja, A., Zohdi, T. I., and Huang, B. (2013). "Anidolic day-light concentrator in structural building envelope." *Proc., 1st Annual Int. Conf. on Architecture and Civil Engineering*, Global Science and Technology Forum (GSTF), Singapore.
- Onaygil, S., and Güler, O. (2003). "Determination of the energy saving by daylight responsive lighting control systems with an example from Istanbul." *Build. Environ.*, 38(7), 973–977.
- Perez, R., Seals, R., Ineichen, P., Stewart, R., and Menicucci, D. (1987). "A new simplified version of the Perez diffuse irradiance model for tilted surfaces." *Sol. Energy*, 39(3), 221–231.
- Radiance 4.2* [Computer software]. Berkeley, CA, Lawrence Berkeley National Laboratory (LBNL).
- Ward, G. J. (1994). "The RADIANCE lighting simulation and rendering system." *Proc., 21st Annual Conf. on Computer Graphics and Interactive Techniques*, Association for Computing Machinery (ACM), New York, 459–472.
- Zohdi, T. I. (2012). "Modeling and simulation of the optical response rod-functionalized reflective surfaces." *Comput. Mech.*, 50(2), 257–268.
- Zubia, J., and Arrue, J. (2001). "Plastic optical fibers: An introduction to their technological processes and applications." *Opt. Fiber Technol.*, 7(2), 101–140.